Microscopic calculation for α and heavier cluster emissions from proton rich Ba and Ce isotopes

A. Florescu[1,2] and A. Insolia[1]
[1]*Department of Physics, University of Catania and INFN, I-95129 Catania, Italy*
[2]*Institute of Atomic Physics, Bucharest, POB MG-6, Romania*
(Received 1 December 1994)

We present a completely microscopic approach for obtaining the preformation factors and the decay widths of α ^{12}C, and ^{16}O cluster decays. We start from realistic single particle Woods-Saxon wave functions and include a large space BCS-type configuration mixing. A pairing interaction acting among valence particles, placed above a double magic core, was considered. The penetrability is evaluated within the WKB approximation. The model predictions are also checked for some well-known α and ^{14}C decays from even-even nuclei.

PACS number(s): 23.60.+e, 23.70.+j, 24.10.−i, 27.60.+j

I. INTRODUCTION

Recently a new region of proton-rich nuclei situated above double-magic ^{100}Sn with masses around $100 < A < 120$ came into the focus of many experimental and theoretical studies. Among other phenomena new types of rare and exotic decays, such as heavier clusters emissions, are expected to be observed here.

As was theoretically predicted more than one decade ago [1,2] and is experimentally established now [3–5] the heavy nuclei with atomic number Z above 86 spontaneously emit heavy clusters ranging from ^{14}C to ^{34}Si and possibly further, the other final nucleus being a close neighbor of the double-magic nucleus ^{208}Pb. It is worth mentioning that also in the spontaneous or thermal neutron-induced cold fission of heavy nuclei from Th to Fm, the highest yields are obtained for splits in which one of the fragments is in the vicinity of ^{132}Sn, which is a double-magic nucleus too [6–8].

The models proposed to describe the heavier cluster emissions could be grouped into phenomenological or fission-type models [9–11] and microscopic models which calculate the decay widths starting from nuclear wave functions given by some nuclear structure model [12–15]. We propose here a microscopic approach, through a generalization of the procedures employed in [14], by introducing realistic single particle (Woods-Saxon) wave functions within an extended configuration-mixing calculation for the nuclear wave functions of the parent and daughter nuclei. The nuclear residual interaction is also taken into account through a pairing interaction which acts between valencelike particles placed above a double-magic core.

II. PREFORMATION AMPLITUDES FOR CLUSTER DECAYS

Considering the emission of cluster a in the decay $B \to A + a$ we wrote the cluster preformation amplitude as

$$F_L(R) = \int d\xi_a d\xi_A d\Omega_R \left[\phi_a(\xi_a)\Psi_A(\xi_A)Y_L(\hat{R})\right]^*_{J_B M_B} \Psi_B(\xi_B) \ , \tag{1}$$

where Ψ_B, Ψ_A, and ϕ_a are the internal wave functions of the initial nucleus, the daughter nucleus, and the emitted cluster, all antisymmetrized and normalized to unity, and ξ_A, ξ_a, are the internal coordinates of the two final nuclei, R being the relative distance between them.

In the present paper we examine the cluster decay of even-even nuclei. The shell model configuration mixing is taken into account through the BCS formalism by introducing a residual pairing interaction which couples pairs of neutrons and protons with zero total spin. In this way the parent nucleus wave function is written as

$$\Psi_B = \sum_{n,p} X(n)X(p) \prod_{n=1}^{q} \mid (n_n l_n j_n)^0_2\rangle \prod_{p=1}^{r} \mid (n_p l_p j_p)^0_2\rangle \Psi_A \ , \tag{2}$$

where $q(r)$ are the number of neutron (proton) pairs in the even-even emitted cluster and the coefficients

$$X(n) = \langle \Psi_B \mid a^\dagger_{\alpha_1} a^\dagger_{-\alpha_1} \cdots a^\dagger_{\alpha_q} a^\dagger_{-\alpha_q} \mid \Psi_A \rangle \ ,$$

$$X(p) = \langle \Psi_B \mid a^\dagger_{\gamma_1} a^\dagger_{-\gamma_1} \cdots a^\dagger_{\gamma_r} a^\dagger_{-\gamma_r} \mid \Psi_A \rangle$$

are expressed in the frame of the second quantization formalism using the particle creation operators $a^\dagger_\alpha$, $a^\dagger_\gamma$ for neutrons and protons, respectively, with $\alpha = \{n_n l_n j_n m_n\}$, $-\alpha = \{n_n l_n j_n - m_n\}$ and $\gamma = \{n_p l_p j_p m_p\}$, $-\gamma = \{n_p l_p j_p - m_p\}$.

The strength of the pairing force was fitted so as to reproduce the experimental pairing gaps or their predicted values taken from calculated nuclear masses [16].

We used realistic single particle wave functions generated in a spherical Woods-Saxon potential and developed in a spherical harmonic oscillator basis with an oscillator parameter α, e.g., for neutrons

$$| (n_n l_n j_n)^0_2\rangle_{\rm WS} = \sum_{\nu_1\nu_2} c_{\nu_1 n_n} c_{\nu_2 n_n} \mid (\nu_1 l_n, \nu_2 l_n)^0_2\rangle_{\rm HO} \ .$$

The parameters chosen for the Woods-Saxon potential were those proposed by Blomqvist and Wahlborn [17].

In order to perform the overlap integral (1), we integrated over the ξ_A coordinates of the daughter nucleus taken as a core, and then transformed the individual coordinates of the last a nucleons forming the cluster into their relative (Jacobi) coordinates (for details see [14]). The cluster wave functions ϕ_a were also expressed in relative coordinates. Further, by integrating on the cluster internal coordinates ξ_a the general expression for the cluster preformation amplitudes resulted as an expansion over the harmonic oscillator radial wave functions $R_{N_{\rm c.m.}0}$ of the relative motion between the two final nuclei,

$$F_0(R) = \sum_{N_{\rm c.m.}} B^{(N_{\rm c.m.})}_{(a)} R_{N_{\rm c.m.}0}\left(A_a \alpha R^2\right) \ , \qquad (3)$$

where A_a is the cluster mass, α the oscillator parameter of the parent nucleus, and $N_{\rm c.m.}$ the oscillator radial quantum number. We performed the calculation of the preformation amplitudes for the alpha, ^{12}C, and ^{16}O clusters. In the case of the alpha emission, the spatial part of the alpha particle wave function is written as usually

$$\phi_\alpha(\xi_\alpha) = \left(\frac{\beta}{\pi}\right)^{9/4} e^{-\beta(\rho_1^2+\rho_2^2+\rho_3^2)/2} \ , \qquad (4)$$

where $\rho_1 = (\mathbf{r_1}-\mathbf{r_2})/\sqrt{2}$, $\rho_2 = (\mathbf{r_3}-\mathbf{r_4})/\sqrt{2}$, $\rho_3 = (\mathbf{r_1}+\mathbf{r_2}-\mathbf{r_3}-\mathbf{r_4})/2$ are the corresponding Jacobi coordinates and the alpha particle oscillator parameter is $\beta = 0.57$ fm^{-2}. The coefficients of the above expansion, Eq. (3), of the cluster preformation amplitude resulted as

$$B^{(N_{\rm c.m.})}_{(4)} = f_n f_p \sum_{j_n, j_p} h(j_n) h(j_p) \sum_{\nu_1\nu_2\pi_1\pi_2} c_{\nu_1 n_n} c_{\nu_2 n_n} c_{\pi_1 n_p} c_{\pi_2 n_p} A^{(N_{\rm c.m.})}_{(4)}(\nu_1 l_n, \nu_2 l_n(0)\pi_1 l_p, \pi_2 l_p(0)0; \alpha, \beta) \ , \qquad (5)$$

and they are formally similar to those obtained earlier by Mang [18] for the overlap integral of the alpha particle using harmonic oscillator single particle wave functions. Here the BCS factors f are

$$f = \prod_j \left(U^i_j U^f_j + V^i_j V^f_j\right)^{\Omega_j} \ ,$$

with $\Omega = (2j+1)/2$ and the i, f superscripts standing for the initial and final nuclei. Also

$$h(j) = \Omega_j \frac{V^i_j U^f_j}{U^i_j U^f_j + V^i_j V^f_j} \ .$$

The coefficients $A^{(N_{\rm c.m.})}_{(4)}(n_1 l_1, n_2 l_2(0) n_3 l_3, n_4 l_4(0)0; \alpha, \beta)$ appear when one calculates the overlap integral Eq. (1) for the case of the alpha particle, using harmonic oscillator single particle wave functions and for a given configuration of the last four particles [14]. When the oscillator parameters α of the harmonic oscillator basis employed for the Woods-Saxon single particle wave functions of the decaying nucleus and the cluster size parameter β are equal, the $A_{(4)}$ coefficients take the very simple expression

$$A^{(N_{\rm c.m.})}_{(4)} = \left(\frac{\pi}{4}\right)^{3/4} \frac{\hat{l}_n \hat{l}_p}{4^{N_{\rm c.m.}}} \left(\frac{N_{\rm c.m.}!(N_{\rm c.m.}+\frac{1}{2})!}{\prod_{i=1}^4 n_i!(n_i+l_i+\frac{1}{2})!}\right)^{1/2} , \qquad (6)$$

with the orbital momenta $l_1 = l_2 = l_n$, $l_3 = l_4 = l_p$ coupled to zero, $\hat{l} = \sqrt{2l+1}$, and the condition

$$N_{\rm c.m.} = n_1 + n_2 + l_n + n_3 + n_4 + l_p .$$

Consequently, in order to simplify the calculation of the overlap integral we used for the harmonic oscillator expansion basis of the Woods-Saxon wave functions a size parameter equal to 0.57 fm^{-2} for the alpha cluster and, respectively, 0.352, 0.330, and 0.306 fm^{-2} for the ^{12}C, ^{14}C, and ^{16}O clusters, values which are consistent with the experimental nuclear mean-square radii of these nuclei. Only $0s$ quantum numbers for the relative motion between pairs of nucleons were considered in the emitted cluster.

In order to calculate the preformation factor of the ^{12}C cluster, we adopted for the ^{12}C internal function the usual ansatz prescribed by the cluster-type nuclear structure theories [19],

$$\phi_{^{12}{\rm C}} = \phi_{\alpha_1}\phi_{\alpha_2}\phi_{\alpha_3}\chi_{20}(\rho_0)\chi_{20}(\rho_r) \ , \qquad (7)$$

where all ϕ_{α_i} are as in Eq. (3) and the two χ_{20} functions describe the relative motions, with four oscillator quanta each, between the first two alpha clusters and, respectively, between their common center of mass and the third alpha cluster: $\chi_{20}(\rho) \sim R_{20}(\beta\rho^2)$. The cluster wave function is normalized to unity with regard to the internal relative coordinates ξ_a.

The coefficients $B_{(a=12)}$ of the preformation amplitude expansion, Eq. (3), are

$$B^{(N_{\rm c.m.})}_{(12)} = \sum_{(s)} B^{(N_{R_1})}_{(4)} B^{(N_{R_2})}_{(4)} B^{(N_{R_3})}_{(4)} J_4(N_{\rho_0}) J_4(N_{\rho_r}) \times \langle N_{\rho_0} N_{R_0} \mid N_{R_1} N_{R_2}\rangle \langle N_{\rho_r} N_{\rm c.m.} \mid N_{R_0} N_{R_3}\rangle \qquad (8)$$

where we denoted the integrals $J_4(N_\rho) = \int_0^\infty R_{N_\rho 0}(\alpha\rho^2)R_{20}(\beta\rho^2)\rho^2 d\rho$ which for the case $\alpha = \beta$ reduce to $J_4 = \delta_{2N_\rho}$. The coefficients $B_{(4)}$ are given by Eq. (5). Here we summed the ensemble of oscillator quantum numbers

$$(s) = \{N_{R_1} N_{R_2} N_{R_3} N_{R_0} N_{\rho_0} N_{\rho_r}\}$$

and $\langle nN \mid n_1 n_2\rangle$ is a shorthand notation for the Moshinsky coefficients [20] with all angular momenta equal to zero. The Moshinsky coefficients were later generalized for the case of unequal-mass particles by Smirnov [21]. In Eq. (8) the second bracket is a generalized Moshinsky coefficient with $D = m_1/m_2 = 2$. We calculated these brackets starting from their expressions given by Trlifaj [22] and Dobes [23]. It must be mentioned that the usual energy-conserving oscillator relations

$$N_{R_0} = N_{R_1} + N_{R_2} - 2, \qquad N_{R_3} = N_{\text{c.m.}} - N_{R_1} - N_{R_2} + 4$$

lower further the number of summing indices in Eq. (8).

Similarly for the ^{16}O preformation amplitude, starting from a cluster-type ^{16}O internal wave function

$$\phi_{^{16}\text{O}} = \phi_{\alpha_1}\phi_{\alpha_2}\phi_{\alpha_3}\phi_{\alpha_4}\chi_{20}(\rho_{01})\chi_{20}(\rho_{02})\chi_{20}(\rho_r) \ , \qquad (9)$$

we obtained the following expression for the corresponding expansion coefficients:

$$B_{(16)}^{(N_{\text{c.m.}})} = \sum_{(s)} B_{(4)}^{(N_{R_1})} B_{(4)}^{(N_{R_2})} B_{(4)}^{(N_{R_3})} B_{(4)}^{(N_{R_4})} \times \langle 2, N_{R_{01}} \mid N_{R_1}, N_{R_2}\rangle \langle 2, N_{R_{02}} \mid N_{R_3}, N_{R_4}\rangle \langle 2, N_{\text{c.m.}} \mid N_{R_{01}}, N_{R_{02}}\rangle \ , \qquad (10)$$

with $(s) = \{N_{R_1} N_{R_2} N_{R_3} N_{R_4} N_{R_{01}} N_{R_{02}}\}$ and taking into account that $J_4(N_{\rho_{01}}) = \delta_{2N_{\rho_{01}}}$, $J_4(N_{\rho_{02}}) = \delta_{2N_{\rho_{02}}}$, $J_4(N_{\rho_r}) = \delta_{2N_{\rho_r}}$ The following oscillator relations are fulfilled:

$$N_{R_{01}} = N_{R_1} + N_{R_2} - 2, \qquad N_{R_{02}} = N_{R_3} + N_{R_4} - 2 \ ,$$

$$N_{R_4} = N_{\text{c.m.}} - N_{R_1} - N_{R_2} - N_{R_3} + 6 \ .$$

In order to compare the predictions of our model with the existing experimental data we calculated also the preformation amplitudes and the decay widths for the ^{14}C emission from some even-even Ra isotopes. We used a cluster wave function

$$\phi_{^{14}\text{C}} = \phi_{\alpha_1}\phi_{\alpha_2}\phi_{\alpha_3}\chi_{00}(\rho_{\nu\nu})\chi_{20}(\rho_{01})\chi_{10}(\rho_{02})\chi_{20}(\rho_r) \ , \qquad (11)$$

where the function χ_{10} indicates that two oscillator quanta are ascribed to the relative motion between the third alpha group and the last pair of neutrons and the function χ_{00} corresponds to the $0s$ internal relative motion among the two neutrons. Finally we obtained

$$B_{(14)}^{(N_{\text{c.m.}})} = \sum_{(s)} B_{(4)}^{(N_{R_1})} B_{(4)}^{(N_{R_2})} B_{(4)}^{(N_{R_3})} B_{(2)}^{(N_{\nu\nu})} \times \langle 2, N_{R_{01}} \mid N_{R_1} N_{R_2}\rangle \langle 1, N_{R_{02}} \mid N_{R_3} N_{\nu\nu}\rangle \langle 2, N_{\text{c.m.}} \mid N_{R_{01}} N_{R_{02}}\rangle \ , \qquad (12)$$

where the coefficients $B_{(2)}$ for the last two neutrons are

$$B_{(2)}^{(N)} = f_n \sum_{j_n} h(j_n) \sum_{\nu_1\nu_2} c_{\nu_1 n_n} c_{\nu_2 n_n} \times A_{(2)}^{(N)}(\nu_1 l_n, \nu_2 l_n(0); \alpha, \beta) \ ,$$

with

$$A_{(2)}^{(N)} = \left(\frac{\pi}{4}\right)^{1/4} \frac{\hat{l}_n}{2^N} \left(\frac{N!(N+\frac{1}{2})!}{\prod_{i=1}^2 n_i!(n_i + l_i + \frac{1}{2})!}\right)^{1/2} \ ,$$

and we observed that $J_2(N_{\rho_{02}}) = \int_0^\infty R_{N_{\rho_{02}} 0}(\alpha\rho_{02}^2)R_{10}(\beta\rho_{02}^2)\rho_{02}^2 d\rho_{02} = \delta_{1N_{\rho_{02}}}$. The energy-conserving relations between the oscillator quantum numbers (s) can be easily deduced from the Moshinsky brackets. Here the second bracket corresponds to a mass ratio equal to 2 and the third one to a mass ratio 4/3.

We should mention that a similar calculation for the decay widths of alpha, ^{12}C, and ^{14}C clusters from Ba and Ra isotopes was made in [15]. The authors also used a BCS configuration-mixing formalism within a large space of spherical single particle wave functions. In Ref. [15] all single particle levels up to the highest considered major shell (N= 18) were included. The agreement between the present calculations and those of Ref. [15] shows that the inclusion of a core ($N = Z = 50$ for the Sn region and $N = 126$, $Z = 82$ for the Pb region) is a good approximation.

TABLE I. The calculated cluster decay widths $\Gamma(R)$ at the matching point R. The Q values were evaluated from [16].

Decay	Q (MeV)	$\Gamma_{\rm th}$ (MeV)	R_c (fm)	$\left(\frac{\Gamma_{\rm cl}}{\Gamma_\alpha}\right)_{\rm th}$
^{114}Ba $\rightarrow ^{12}$ C $+^{102}$ Sn	20.62	0.89(-25)	10.3	1.7(-1)
$\rightarrow \alpha+^{110}$Xe	3.44	0.53(-24)	8.5	
^{116}Ba $\rightarrow ^{12}$ C$+^{104}$Sn	17.00	0.10(-32)	10.4	9.1(-6)
$\rightarrow \alpha+^{112}$Xe	2.96	0.11(-27)	8.5	
^{118}Ba $\rightarrow ^{12}$ C$+^{106}$Sn	15.10	0.42(-38)	10.5	1.6(-5)
$\rightarrow \alpha+^{114}$Xe	2.41	0.26(-33)	8.5	
^{116}Ce $\rightarrow ^{16}$ O$+^{100}$Sn	30.10	0.18(-25)	10.8	5.5(-2)
$\rightarrow ^{12}$ C$+^{104}$Te	18.87	0.41(-30)	10.4	1.2(-6)
$\rightarrow \alpha+^{112}$Ba	3.59	0.33(-24)	8.5	
^{118}Ce $\rightarrow ^{16}$ O$+^{102}$Sn	29.26	0.11(-26)	10.9	2.8
$\rightarrow ^{12}$ C$+^{106}$Te	17.77	0.96(-33)	10.5	2.4(-6)
$\rightarrow \alpha+^{114}$Ba	3.19	0.40(-27)	8.5	
^{120}Nd $\rightarrow ^{16}$ O$+^{104}$Te	29.35	0.14(-28)	10.9	7.0(-2)
$\rightarrow \alpha+^{116}$Ce	3.32	0.20(-27)	8.5	

III. CALCULATION OF CLUSTER DECAY WIDTHS

We evaluated the cluster decay widths in the frame of the R-matrix theory,

$$\Gamma_{\rm cl}(R) = \sum_L P_L(R)\gamma_L^2(R) = \frac{\hbar^2 R}{2M}\sum_L P_L(R) \mid F_L(R) \mid^2 , \tag{13}$$

as a function of the channel radius R.

The penetrability factor P for the spherical potential barrier between the final fragments was obtained within the WKB approximation using pure Coulomb wave functions,

$$P_L(R) = \frac{2kR}{G_L^2(kR) + F_L^2(kR)} , \tag{14}$$

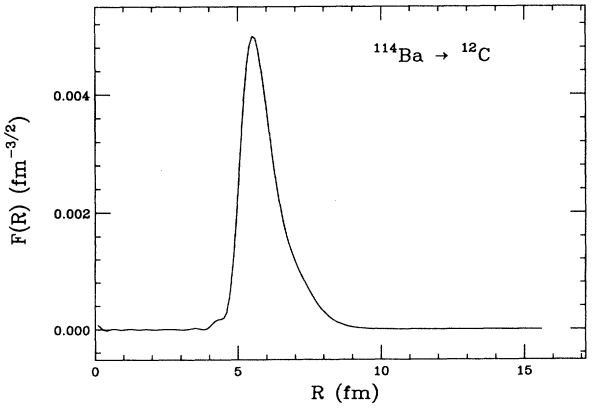

FIG. 1. The preformation factor $F(R)$ for the emission of ^{12}C from ^{114}Ba as a function of the distance R between the two final nuclei.

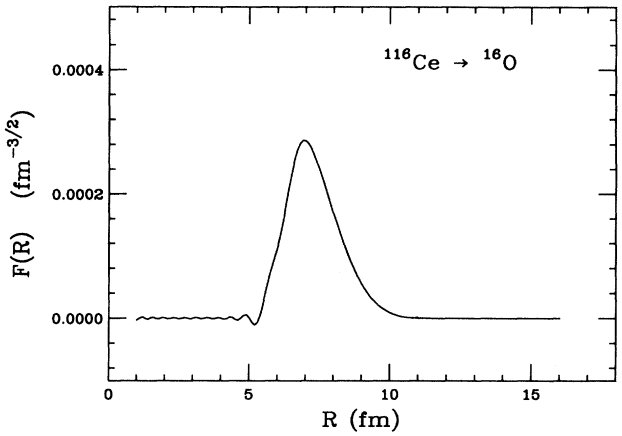

FIG. 2. The preformation factor $F(R)$ for the emission of ^{16}O from ^{116}Ce as a function of the relative distance R.

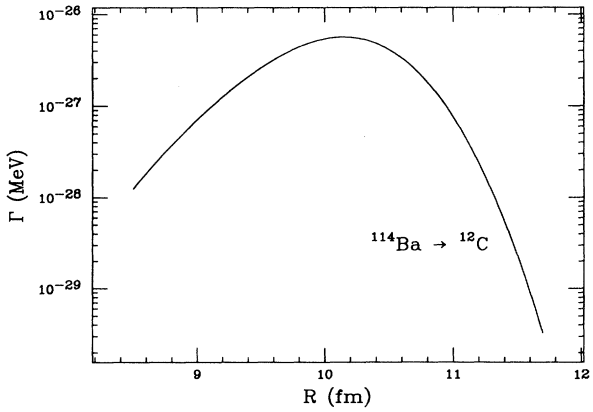

FIG. 3. The decay width Γ for the emission of ^{12}C from ^{114}Ba as a function of the relative distance R.

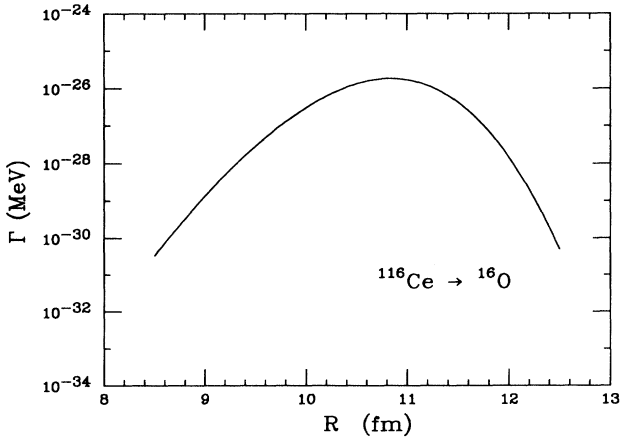

FIG. 4. The decay width Γ for the emission of ^{16}O from ^{116}Ce as a function of the relative distance R.

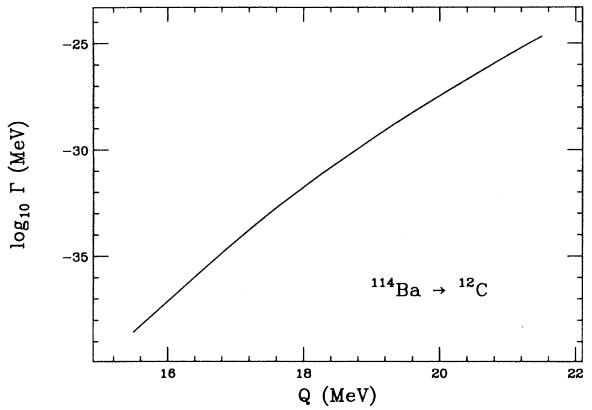

FIG. 5. The logarithm of the decay width for the emission of ^{12}C from ^{114}Ba as a function of the decay Q value.

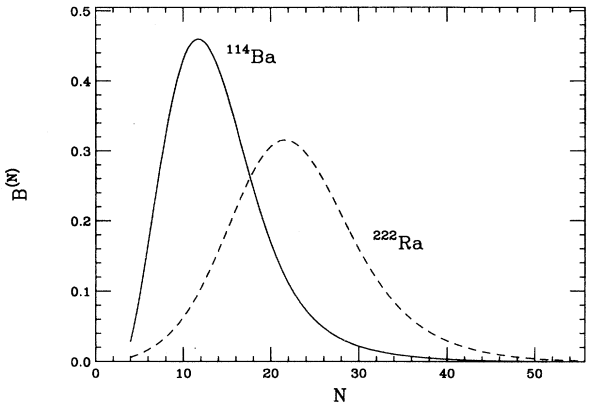

FIG. 6. The coefficients $B^{(N)}_{(4)}$ calculated from Eq. (5) for the alpha emission from ^{114}Ba and ^{222}Ra, respectively, as a function of the oscillator quantum number N of the center of mass motion of the alpha cluster.

where $k = (1/\hbar)\sqrt{2QA_a}$.

In Table I the calculated decay widths for the alpha, ^{12}C, and ^{16}O cluster emissions from some proton-rich Ba, Ce, and Nd isotopes are presented. The highest major shell included in the calculation was $N = 18$. We used for the gap parameters an average value of 1.15 MeV for neutrons and 1.30 MeV for protons. The Q values were extracted from the mass predictions of Janecke and Masson [16] for this region. In Figs. 1 and 2 we show the preformation amplitudes $F_0(R)$ for the heavier clusters ^{12}C and ^{16}O emitted from ^{114}Ba and ^{116}Ce, respectively, which have characteristic strong maxima at the nuclear surface. In Figs. 3 and 4 the corresponding decay widths are presented. One can observe that the $\Gamma_{\rm cl}$ values are approximately constant within an order of magnitude, on a large interval of values of the channel coordinate R. This interval is placed about 1 – 2 fm outside the touching radius R_t between the two final nuclei: For example, for $R_t = 1.2(A^{1/3} + a^{1/3})$ we obtain 8.3 fm for ^{102}Sn + ^{12}C and 7.7 fm for ^{110}Xe+α.

In Fig. 5 the calculated decay width for the ^{12}C emission from ^{114}Ba is given as function of the Q value, since the experimental value of this decay is not yet known.

Figure 6 shows the $B^{(N)}_{(4)}$ coefficients corresponding to the alpha decay of ^{114}Ba and ^{222}Ra. One can see that the main contribution to the alpha preformation amplitude comes from those terms with center of mass quantum numbers N for the alpha cluster corresponding to four nucleons situated in a few major shells above the double-magic core, that is, $\Lambda = 4 - 6$ oscillator quanta each in the first case, $\Lambda = 5 - 7$ for protons, and $\Lambda = 6 - 8$ for neutrons in the second case while the harmonic oscillator relation $2N + L = \sum_{i=1}^{4} \Lambda_i = \sum_{i=1}^{4}(2n_i + l_i)$ is fulfilled.

In order to check the accuracy of our theory, we also calculated the alpha and ^{14}C decay widths for some nuclei with experimentally known Γ_α [24] and $\Gamma_{\rm cl}$ [4] values. They are compared in Table II. As alpha emitters we selected mainly spherical nuclei. Here the model reproduces well the experimental decay widths, typically within a factor ranging from 2 to 4, with the exception of the ^{212}Po alpha decay. For the actinide region the highest major shell taken into consideration was $N = 20$ while the inert double-magic core was that of ^{208}Pb. The input values for the gap parameters were obtained from the experimental masses, e.g., $\Delta_n = 0.73$ MeV, $\Delta_p = 1.04$ MeV for ^{222}Ra.

The calculated cluster decay widths are strongly dependent on the corresponding Q values, due to the penetrability factor P. In order to illustrate this dependence we present in Table III the half-lives $T_{1/2} = 0.693\hbar/\Gamma$

TABLE II. The experimental and calculated values of cluster decay widths Γ for some well-studied cases. The Q values are the experimental ones.

Decay	Q (MeV)	$\Gamma_{\rm expt}$ (MeV)	$\Gamma_{\rm th}$ (MeV)	R_c (fm)
^{106}Te → α+^{102}Sn	4.32	0.76(-17)	0.33(-17)	8.2
^{146}Sm → α+^{142}Nd	2.54	0.15(-36)	0.77(-37)	8.1
^{148}Gd → α+^{144}Sm	3.29	0.20(-30)	0.12(-30)	8.1
^{212}Po → α+^{208}Pb	8.96	0.15(-14)	0.17(-15)	8.8
^{218}Rn → α+^{214}Po	7.27	0.13(-19)	0.30(-20)	9.0
^{222}Ra → α+^{218}Rn	6.68	0.12(-22)	0.47(-23)	9.0
^{222}Ra →^{14} C+^{208}Pb	33.05	0.41(-32)	0.25(-33)	11.9

for the alpha, ^{12}C, and ^{16}O cluster decays from the same proton-rich Ba, Ce, and Nd isotopes, estimated at three different decay energies for each case. Some of these decay energies are predicted by the mass calculations of Janecke and Masson [16] and others by the recent extended calculations of Möller *et al.* [25]. The Q values that we chose cover also the extremities of the decay energy predictions, thus pointing to the possible range for the cluster decay half-lives. Other $T_{1/2}$ estimations for the same decays could be deduced as function of the Q values, through a direct interpolation from Table III.

TABLE III. The calculated cluster half-lives $T_{1/2}$ at three different decay energies.

Decay	Q (MeV)		$T_{1/2}$(s)
^{114}Ba $\rightarrow^{12}$ C+^{102}Sn	19.00		0.87 (7)
	20.62	[16]	0.51 (4)
	21.44	[25]	0.18 (3)
$\rightarrow \alpha$+^{110}Xe	2.00		0.74(18)
	3.44	[16]	0.87 (3)
	5.00		0.95(-5)
^{116}Ba $\rightarrow^{12}$ C+^{104}Sn	15.50		0.80(16)
	17.00	[16]	0.45(12)
	19.00		0.80 (7)
$\rightarrow \alpha$+^{112}Xe	2.40	[25]	0.22(13)
	2.96	[16]	0.43 (7)
	4.00		0.32
^{118}Ba $\rightarrow^{12}$ C+^{106}Sn	14.00		0.63(21)
	15.10	[16]	0.11(18)
	16.50		0.74(13)
$\rightarrow \alpha$+^{114}Xe	1.90	[25]	0.35(20)
	2.41	[16]	0.18(13)
	3.50		0.35 (3)
^{116}Ce $\rightarrow^{16}$ O+^{100}Sn	27.00		0.33(10)
	30.10	[16]	0.25 (5)
	32.00	[25]	0.55 (2)
$\rightarrow^{12}$ C+^{104}Te	16.00		0.43(17)
	18.87	[16]	0.11(10)
	20.12	[25]	0.22 (7)
$\rightarrow \alpha$+^{112}Ba	3.07	[25]	0.12 (8)
	3.59	[16]	0.14 (4)
	4.50		0.11(-1)
^{118}Ce $\rightarrow^{16}$ O+^{102}Sn	27.00		0.28(10)
	29.26	[16]	0.40 (6)
	31.00		0.10 (4)
$\rightarrow^{12}$ C+^{106}Te	15.00		0.67(20)
	17.77	[16]	0.47(12)
	19.00		0.53 (9)
$\rightarrow \alpha$+^{114}Ba	1.95	[25]	0.34(21)
	3.19	[16]	0.12 (7)
	4.00		0.41 (1)
^{120}Nd $\rightarrow^{16}$ O+^{104}Te	27.00		0.53(12)
	29.35	[16]	0.32 (8)
	31.00		0.82 (5)
$\rightarrow \alpha$+^{116}Ce	1.96	[25]	0.18(23)
	3.32	[16]	0.23 (7)
	4.50		0.12

Finally we compared our calculated cluster decay widths for the region of proton-rich Ba and Ce isotopes, with those resulting from the simplified semimicroscopic model of Blendowske *et al.* [26] which includes a "bulk" spectroscopic factor and a penetrability through the nuclear plus Coulomb barrier given by the Christensen-Winther potential [27]. The latter values are 2 – 5 times lower than ours for the same Q values, for alpha decay, and a spectroscopic factor $S_{\rm bulk} = 0.63 \times 10^{-2}$, and more than 10^2 times lower for the ^{12}C emission and a spectroscopic factor $S_{\rm bulk} = 10^{-8}$. This difference could indicate that the "bulk" spectroscopic factor is in fact dependent not only on the mass of the cluster but also on the mass ratio between the two final nuclei. We are prepared to examine more thoroughly this point in another paper.

IV. CONCLUSIONS

We presented here a microscopic treatment for the calculation of the cluster preformation factors and decay widths, using single particle wave functions generated by a realistic nuclear mean field and introducing a large-scale configuration mixing through a residual pairing interaction. In this way earlier drastic approximations such as restricting to harmonic oscillator single particle wave functions and restricting to a few single particle configurations [14] were avoided. This formalism allowed us to obtain explicit expressions for the preformation amplitudes of heavy clusters such as ^{12}C, ^{14}C, and for the first time ^{16}O, and it could also permit one to calculate with a reasonable degree of approximation the preformation factors for even heavier clusters. For the time being we examined only the cluster decays of even-even nuclei.

We neglected in our calculations the influence of the nuclear deformation on the calculated penetrabilities, for some cases such as the alpha and ^{14}C emissions from Ra isotopes. Estimates of this effect [10,15,28] show that it could contribute up to a factor of 10 to the final values of the alpha and heavier cluster decay widths.

The present calculations can be extended in a straightforward way to deformed nuclei, and also to more elaborate and realistic internal wave functions for the emitted heavier clusters. Also a problem which needs further study is the influence of the antisymmetrization effects on the cluster preformation amplitudes in the region of the nuclear surface behind the touching point.

ACKNOWLEDGMENTS

The authors wish to thank R. Bonetti, D. Delion, A. Guglielmetti, R. J. Liotta and A. Sandulescu for helpful discussions. One of us (A.F.) is grateful for the support received from the Commission of the European Communities and the European East–West Science Mobility Program, under Contract No. ERB3510PL922207, and also wishes to thank the University of Catania and I.N.F.N., Sezione di Catania, for their support and kind hospitality.

[1] A. Sandulescu and W. Greiner, J. Phys. G **3**, L189 (1977).
[2] A. Sandulescu, D.N. Poenaru, and W. Greiner, Sov. J. Part. Nucl. Phys. **11**, 528 (1980).
[3] H.J. Rose and G.A. Jones, Nature **307**, 245 (1984).
[4] P.B. Price, Nucl. Phys. **A502**, 41c (1989).
[5] R. Bonetti and A. Guglielmetti, in *Handbook of Nuclear Decay Modes,* edited by D. N. Poenaru and W. Greiner (Institute of Physics, Bristol, England, in press).
[6] H.-G. Clerc, W. Lang, M. Mutterer, C. Schmitt, J.P. Theobald, U. Quade, K. Rudolf, P. Ambruster, F. Goennenwein, H. Schrader, and P. Engelhard, Nucl. Phys. **A452**, 277 (1986).
[7] A. Sandulescu and W. Greiner, Rep. Prog. Phys. **55**, 1423 (1992).
[8] F. Goennenwein *et al.*, in *Frontier Topics in Nuclear Physics*, NATO Advanced Study Institute, Series B: Physics, edited by W. Scheid and A. Sandulescu (Plenum, New York, in press).
[9] D.N. Poenaru, M. Ivascu, A. Sandulescu, and W. Greiner, Phys. Rev. C **32**, 572 (1985); D.N. Poenaru *et al.*, At. Data Nucl. Data Tables **34**, 423 (1986).
[10] Y.-J. Shi and W.J. Swiatecki, Nucl. Phys. **A438**, 450 (1985); **A464**, 205 (1987).
[11] B. Buck, A.C. Merchant, and S.M. Perez, J. Phys. G **15**, 615 (1989); At. Data Nucl. Data Tables **54**, 53 (1993).
[12] R. Blendowske, T. Fliessbach, and H. Walliser, Nucl. Phys. **A464**, 75 (1987).
[13] M. Ivascu and I. Silisteanu, Nucl. Phys. **A485**, 93 (1988).
[14] A. Florescu, S. Holan, and A. Sandulescu, Rev. Roum. Phys. **33**, 131 (1988); **33**, 243 (1988); **34**, 595 (1989).
[15] D. Delion, A. Insolia, and R.J. Liotta, J. Phys. G **19**, L189 (1993); **20**, 1483 (1994).
[16] J. Janecke and P.J. Masson, At. Data Nucl. Data Tables **39**, 266 (1988).
[17] J. Blomqvist and S. Wahlborn, Ark. Fys. **16**, 545 (1960).
[18] H.J. Mang, Annu. Rev. Nucl. Sci. **14**, 1 (1964).
[19] K. Wildermuth and Th. Kanellopoulos, Nucl. Phys. **7**, 158 (1958); **8**, 449 (1958); K. Wildermuth and Y.C. Tang, *A Unified Theory of the Nucleus* (Vieweg, Braunschweig, 1977).
[20] M. Moshinsky, Nucl. Phys. **13**, 104 (1959).
[21] Yu.F. Smirnov, Nucl. Phys. **27**, 177 (1961); **39**, 346 (1962).
[22] L. Trlifaj, Phys. Rev. C **5**, 1534 (1972).
[23] J. Dobes, J. Phys. A **10**, 2053 (1977).
[24] A. Rytz, At. Data Nucl. Data Tables **47**, 205 (1991).
[25] P. Möller, J.R. Nix, W.D. Myers, and W.J. Swiatecki, At. Data Nucl. Data Tables **59**, 185 (1995).
[26] R. Blendowske, T. Fliessbach, and H. Walliser, Z. Phys. A **339**, 121 (1991).
[27] P.R. Christensen and A. Winther, Phys. Lett. **65B**, 19 (1976).
[28] D.S. Delion, A. Insolia, and R.J. Liotta, Phys. Rev. C **46**, 1346 (1992).